AADE-06-DF-HO-45

Generalized Hydraulic Calculation Method for Flow of Non-Newtonian Fluids in Eccentric Annuli

Ali Pilehvari and Robert Serth, Department of Chemical and Natural Gas Engineering, Texas A&M University-Kingsville

Abstract

The flow of non-Newtonian fluids through eccentric annuli is prevalent during drilling and cementing operations of directional and horizontal wells. The flow pattern in an eccentric annulus can differ greatly from that in a concentric annulus, and this difference affects both the pressure drop and the laminar-turbulent transition point. When the flow regime is the same, either laminar or turbulent, in both geometries, the pressure drop is much lower in a fully eccentric annulus. However, the transition from laminar to turbulent flow begins at a lower flow rate in an eccentric annulus. Therefore, the pressure drop may be higher in an eccentric annulus under certain conditions. Errors resulting from ignoring the effect of eccentricity on frictional pressure drop and equivalent circulating density can lead to formation fracture or well control problems in some situations.

In this paper a new method is presented for calculating pressure losses in eccentric annuli. The method is based on an effective diameter that accounts for the effects of both conduit geometry and fluid rheology. Predictions of the method are compared with an extensive set of data for drilling fluids obtained from a large-scale flow loop. The results demonstrate that the new method is capable of reliably predicting the pressure drop of most drilling fluids in both laminar and turbulent flow regimes for eccentric annular geometries of practical interest.

Introduction

The flow of non-Newtonian fluids through eccentric annuli occurs during drilling and cementing operations for oil and gas wells. Approximate and exact (numerical) solutions to the fundamental flow equations in this geometry have been published for Bingham plastic, power-law and yield-power-law fluids. The purpose of this article is to present a generalized method for computing frictional pressure losses in eccentric annuli that is applicable to a wide variety of drilling fluids. Predictions obtained with the new method are compared with experimental data from a large flow loop that are available in the literature.

An eccentric annulus is shown in cross-section in **Fig. 1**, where R_1 and R_2 are the radii of the inner and outer cylinders, respectively, and δ is the center-to-center distance between the two cylinders. The eccentricity, *e*, is defined as:

$$e = \frac{\delta}{R_2 - R_1} = \frac{2\,\delta}{D_2 - D_1} \qquad \ldots(1)$$

The eccentricity ranges from zero to unity, with $e = 0$ corresponding to a concentric annulus and $e = 1$ corresponding to a fully eccentric annulus (inner cylinder in contact with outer cylinder).

The flow pattern in an eccentric annulus can differ greatly from that in a concentric annulus (Haciislamoglu and Langlinais, 1990; Fang et al., 1999), and this difference affects both the pressure drop and the laminar-turbulent transition point. When the flow regime is the same (either laminar or turbulent) in both geometries, the pressure drop is lower in the eccentric annulus. For example, in laminar Newtonian flow the pressure drop in a fully eccentric annulus can be as low as 40% of that in an equivalent concentric annulus at the same flow rate (Haciislamoglu and Cartalos, 1994). However, the transition to turbulent flow begins at a lower Reynolds number in an eccentric annulus. Therefore, the pressure drop may be higher in an eccentric annulus under certain conditions, for example, when the flow is turbulent in the eccentric geometry but remains laminar in the concentric geometry (Haciislamoglu and Cartalos, 1994). The situation is thus complex, and neglecting the effects of eccentricity can result in serious errors.

Prior Work

Flow in eccentric annuli has been of interest for many years, and a fairly extensive literature exists on the subject. An extensive bibliography of work dealing with

laminar non-Newtonian flow in annular channels is presented by Escudier et al. (2002). The discussion here is limited to research that is of most relevance to the present work.

An analytical solution of the Navier-Stokes equations for laminar Newtonian flow in an eccentric annulus was obtained by Snyder and Goldstein (1965). Although rather complicated, the solution can be used to compute geometrical parameters for eccentric annuli. Guckes (1975) obtained numerical solutions to the fundamental equations of motion for laminar flow of Bingham plastic and power-law fluids in eccentric annuli. The results were presented graphically for limited ranges of parameters, and hence are not very suitable for use in the present context. Haciislamoglu and Langlinais (1990) numerically solved the equations of motion for laminar flow of Bingham plastic, power-law and yield-power-law fluids in eccentric annuli. The results for power-law fluids were presented in the form of a regression equation for the ratio, R, of frictional pressure gradient in an eccentric annulus to that in a concentric annulus.

$$R = 1 - 0.072\,(e/n)\sigma^{0.8454} - 1.5\,e^2\sqrt{n}\,\sigma^{0.1852} + 0.96\,e^3\sqrt{n}\,\sigma^{0.2527} \quad \ldots(2)$$

where $R = (\Delta P/\Delta L)_{EA}/(\Delta P/\Delta L)_{CA}$

$n =$ exponent in power-law model

$\sigma = D_1/D_2$

$D_1 =$ OD of inner cylinder

$D_2 =$ ID of outer cylinder

$EA =$ eccentric annulus

$CA =$ concentric annulus

Eq. 2 is valid (to within 5%) for the following parameter ranges:

$$0.3 \le \sigma \le 0.9$$
$$0 \le e \le 0.95$$
$$0.4 \le n \le 1.0$$

The range for σ covers most practical applications, and the correlation can be extrapolated to include the fully eccentric annulus ($e = 1.0$) with little error. Thus, the only limitation of practical significance is the range of n.

Eq. 2 is a very useful relationship. Setting $n = 1$ provides a simple solution for the pressure drop in laminar Newtonian flow in eccentric annuli. This solution is much more convenient to use than the solution of Snyder and Goldstein (1965) mentioned above. Furthermore, **Eq. 2** offers the possibility of generalization to non-power-law fluids by replacing the power-law exponent, n, with the generalized power-law exponent, n'.

Haciislamoglu and Cartalos (1994, 1996) showed that **Eq. 2** can be used for skewed annuli by replacing the eccentricity with an appropriate average value. They also gave critical Reynolds numbers for skewed and uniformly eccentric annuli, and a modification of **Eq. 2** for turbulent flow.

Reed and Sas-Jaworsky (1996) used Equation (2) to define an effective diameter for the flow of power-law fluids in eccentric annuli. Pressure drop calculations based on this diameter showed good agreement with experimental data for power-law fluids in both laminar and turbulent flow regimes.

Fang et al. (1999) and Escudier et al. (2002) obtained numerical solutions to the equations of motion for the laminar flow of power-law fluids in eccentric annuli with power-law exponents in the range 0.2 to 1.0. The latter authors also studied the effects of inner cylinder rotation. Where the two studies overlap, the results are generally in close agreement with one another. For n = 0.2, however, there are discrepancies at small values of eccentricity. The difficulty in obtaining numerical solutions for small values of n is acknowledged by Fang et al. (1999). They did not obtain solutions for n< 0.2 due to the very large computing times required for these cases.

Miller's Hypothesis

Miller (1972) proposed that the flow-rate-pressure-drop relationship in laminar flow of any time-independent fluid in a conduit of arbitrary cross-section can be characterized by a single geometrical parameter, *S*, that is independent of fluid rheology. This parameter allows the conduit to be treated as an equivalent pipe. Hanks (1974) analyzed the validity of this concept for Bingham plastic and power-law fluids flowing in conduits with several simple geometries. Miller's hypothesis can be stated in terms of an equivalent diameter, D_{eq}, defined by **Eq. 3** and related through Eq. 4 to the parameter, S, which is given by Eq. 5.

$$\bar{\gamma}_N = 8V/D_{eq} \quad \ldots(3)$$
$$D_{eq} = 16\,D_h/S \quad \ldots(4)$$
$$S = f_N\,\mathrm{Re}_N \quad \ldots(5)$$

where

$\bar{\gamma}_N =$ average Newtonian shear rate at conduit wall

$V =$ average fluid velocity

$D_h =$ hydraulic diameter =4×flow area /wetted perimeter

$f_N =$ Fanning friction factor for laminar Newtonian flow in the given geometry

$\mathrm{Re}_N = D_h V \rho/\mu =$ Newtonian Reynolds number

$\rho, \mu =$ density and viscosity of Newtonian fluid

Note that since *S* is independent of rheology, it can be determined from the friction-factor-Reynolds-number relationship for Newtonian flow in the given geometry, which can be based on a solution of the Navier-Stokes equations or on experimental data.

For a circular pipe of diameter, *D*:

$$S = f_N \mathrm{Re}_N = 16 \quad \ldots(6)$$

$$D_h = D \quad \ldots(7)$$

$$D_{eq} = D \quad \ldots(8)$$

Thus, the general equations reduce to the correct result for pipe flow.

For a concentric annulus, the exact solution to the Navier-Stokes equations yields the following results (Miller, 1972):

$$S = f_N \mathrm{Re}_N = \frac{16(1-\sigma)^2}{[1+\sigma^2+(1-\sigma^2)/\ln\sigma]} \quad \ldots(9)$$

$$D_h = D_2 - D_1 \quad \ldots(10)$$

$$D_{eq} = \frac{D_h[1+\sigma^2+(1-\sigma^2)/\ln\sigma]}{(1-\sigma)^2} = \frac{D_L^2}{D_h} \quad \ldots(11)$$

where

$$D_L = \left\{D_2^2 + D_1^2 - (D_2^2 - D_1^2)/\ln\sigma\right\}^{1/2} \quad \ldots(12)$$

$= $ Lamb's diameter

The equivalent diameter defined by **Eq.11** has been used in a generalized hydraulic calculation method by Pilehvari and Serth (2005). It gives excellent agreement with experimental data for laminar flow of drilling fluids in concentric annuli, and usually provides reliable results for turbulent flow as well. Thus, Miller's method is consistent with experimental results for flow in concentric annuli.

The above development can be extended to an eccentric annulus using the pressure drop ratio, R_N, for a Newtonian fluid. Setting $n = 1$ in **Eq. 2** yields:

$$R_N = 1 - 0.072\, e\, \sigma^{0.8454} - 1.5 e^2 \sigma^{0.1852} + 0.96 e^3 \sigma^{0.2527} \quad \ldots(13)$$

$$f_{N,EA} = R_N\ f_{N,CA} \quad \ldots(14)$$

From **Eqs. 9, 11** and **14**, the following results for an eccentric annulus are obtained:

$$S = \frac{16 R_N (1-\sigma)^2}{[1+\sigma^2+(1-\sigma^2)/\ln\sigma]} \quad \ldots(15)$$

$$D_{eq} = \frac{D_L^2}{R_N D_h} \quad \ldots(16)$$

The validity of Miller's hypothesis for flow in eccentric annuli was tested using rheological data for two polymer solutions studied by Haciislamoglu and Cartalos (1994). The rheograms of these fluids are well represented by the power-law model with exponents of 0.75 and 0.55, respectively. Pressure drops were calculated for laminar flow in annuli with different eccentricities and fixed inner and outer diameters of 18 *mm* and 24 *mm*, respectively. The calculations were made by treating the annulus as an equivalent pipe of diameter D_{eq} computed from **Eq. 16**.

The (essentially) exact pressure drops were obtained using **Eq. 2** in conjunction with the analytical solution for laminar flow of a power-law fluid in a concentric annulus (Chhambra and Richardson, 1997):

$$Q = \frac{\pi n D_2^3}{8(3n+1)}\left(\frac{D_2 \Delta P}{4KL}\right)^{1/n} * \left\{(1-\lambda^2)^{(n+1)/n} - \sigma^{(n-1)/n}(\lambda^2-\sigma^2)^{(n+1)/n}\right\} \quad \ldots(17)$$

In this equation *Q* is the volumetric flow rate, L is the conduit length, *K* is the coefficient in the power-law model and λ is the dimensionless radial position at which the fluid velocity is maximum. It is found by solving the following integral equation:

$$\int_\sigma^\lambda \left(\frac{\lambda^2}{x} - x\right)^{1/n} dx = \int_\lambda^{1.0} \left(x - \frac{\lambda^2}{x}\right)^{1/n} dx \quad \ldots(18)$$

Figs. 2-5 show the solutions for the fluid with $n = 0.55$ in annuli of different eccentricities. For the concentric annulus, the two solutions agree quite well, but the agreement deteriorates with increasing eccentricity. **Fig. 6** shows solutions for the fluid with $n = 0.75$ in a highly eccentric annulus ($e = 0.95$). Comparing **Figs. 5** and **6**, it is seen that the agreement between approximate and exact solutions deteriorates as *n* decreases. (Note that the two solutions coincide for

$n = 1$). Thus, Miller's hypothesis does not provide a suitable basis for calculating pressure losses in eccentric annuli for non-Newtonian fluids.

From the above results it is clear that if a single parameter is to be used to characterize the flow-rate-pressure-drop relationship in eccentric annuli, it must include the effect of fluid rheology as well as the conduit geometry.

Effective Diameter for Eccentric Annuli

In order to overcome the inherent limitation of Miller's method, it is proposed to characterize the flow-rate-pressure-drop relationship in eccentric annuli by using the power-law solution rather than the Newtonian solution. To this end, Equation (17) is recast in terms of friction factor and Reynolds number by making the following substitutions:

$$\Delta P = 4 L \tau_w / D_h \qquad \ldots(19)$$

$$\tau_w = \frac{f \rho V^2}{2 g_c} \qquad \ldots(20)$$

$$Q = V A = V(\pi/4)\left(D_2^2 - D_1^2\right) \qquad \ldots(21)$$

After some algebraic manipulation, the result is:

$$f \left\{ \frac{\omega D_2^{(3n+1)/n}}{(D_1 + D_2) D_h^{(n+1)/n}} \right\}^n \frac{V^{2-n} \rho}{8^{(n-1)} g_c K \left[(3n+1)/4n\right]^n} = 16 \qquad \ldots(22)$$

where

$$\omega = \left(1 - \lambda^2\right)^{(n+1)/n} - \sigma^{(n-1)/n}\left(\lambda^2 - \sigma^2\right)^{(n+1)/n} \qquad \ldots(23)$$

The effective diameter for a power-law fluid in a concentric annulus is now defined as:

$$D_{eff,PL,CA} = \frac{\omega D_2^{(3n+1)/n}}{(D_1 + D_2) D_h^{(n+1)/n}} \qquad \ldots(24)$$

Equation (22) can then be written as:

$$f \, \mathrm{Re}_{PL} = 16 \qquad \ldots(25)$$

where the Reynolds number for a power-law fluid is given by:

$$\mathrm{Re}_{PL} = \frac{D_{eff}^n V^{2-n} \rho}{8^{(n-1)} g_c K \left[(3n+1)/4n\right]^n} \qquad \ldots(26)$$

For a power-law fluid in an eccentric annulus, Equation (14) becomes:

$$f_{PL,EA} = R \, f_{PL,CA} \qquad \ldots(27)$$

From this relationship, it follows that Equations (25) and (26) will hold for an eccentric annulus if the effective diameter given by Equation (24) is divided by a factor of $R^{1/n}$, i.e.,

$$D_{eff,PL,EA} = \frac{\omega D_2^{(3n+1)/n}}{(D_1 + D_2) D_h^{(n+1)/n} R^{1/n}} \qquad \ldots(28)$$

This result differs from the effective diameter defined by Reed and Sas-Jaworsky (1996), who based their development on the flow rate versus pressure drop relationship for laminar Newtonian flow in a concentric annulus rather than **Eq. 17**.

The above development can be extended to a generalized power-law fluid by assuming the flow curve has the following form, where τ_w is the wall shear stress:

$$\tau_w = K' \left(8V/D_{eff}\right)^{n'} \qquad \ldots(29)$$

The following substitutions are now made in the above equations for a power-law fluid:

$$n = n' \qquad \ldots(30)$$

$$K\left(\frac{3n+1}{4n}\right)^n = K' \qquad \ldots(31)$$

Eqs. 25, 26 and **28** then become:

$$f \, \mathrm{Re}_G = 16 \qquad \ldots(32)$$

$$\mathrm{Re}_G = \frac{D_{eff}^{n'} V^{2-n'} \rho}{8^{(n'-1)} g_c K'} \qquad \ldots(33)$$

$$D_{eff} = \frac{\omega' D_2^{(3n'+1)/n'}}{(D_1 + D_2) D_h^{(n'+1)/n'} (R')^{1/n'}} \qquad \ldots(34)$$

In these equations, Re_G is the generalized Reynolds number and R' and ω' are given by **Eqs. 2** and **23**, respectively, with n replaced by n'. The effective diameter given by **Eq. 34** is to be used in place of the

equivalent diameter of **Eq. 16** for calculating the pressure drop in an eccentric annulus.

Hydraulic Calculation Procedure

The hydraulic calculation method of Pilehvari and Serth (2005) can be modified to incorporate the effective diameter for eccentric annuli given by **Eq. 34**. The method, outlined below, utilizes the rational polynomial (RP) rheological model, but other models such as yield-power-law, Sisko, etc. can be used as well. Since the effective diameter depends on n', an iterative loop is required to calculate n' and D_{eff}. The necessary steps are described in the following:

Step 1. Calculation of the Flow Curve

The Rabinowitsch-Mooney equation (Govier and Aziz, 1972) is used with the pipe diameter replaced by the effective diameter.

$$8V / D_{eff} = \left(4/\tau_w^3\right) \int_0^{\gamma_w} \tau^3 \gamma \left(d\tau/d\gamma\right) d\gamma \qquad \ldots(35)$$

where

$\gamma =$ true shear rate

$\gamma_w =$ true shear rate at conduit wall

$\tau =$ shear stress

The rheological model is used to express τ and $d\tau / d\gamma$ in terms of γ, and the integral is evaluated numerically to obtain a table of τ_w vs. $8V / D_{eff}$.

Step 2. Cubic Spline

A cubic spline is fitted to the $\ln \tau_w$ vs. $\ln(8V / D_{eff})$ data from Step 1. This spline is used to represent the flow curve in all subsequent calculations.

Step 3. Calculation of n' and D_{eff}

For a given flow rate, *Q*, the average velocity, *V*, is calculated from **Eq. 21**. The iterative loop is initialized by setting $n' = 1.0$.

Step 3a. Eq. 18 is solved to obtain the value of *λ*. The integrals are evaluated numerically and a bounded secant method is used as the equation solver. Note that $\sigma \le \lambda \le 1.0$.

Step 3b. Eq. 2 is used with *n* replaced by n' to calculate R'.

Step 3c. Eq. 34 is used to calculate D_{eff}, from which the value of $8V / D_{eff}$ is obtained.

Step 3d. The value of n' is given by:

$$n' = \frac{d \ln \tau_w}{d \ln (8V / D_{eff})} \qquad \ldots(36)$$

The derivative is computed by differentiating the cubic spline at the value of $8V / D_{eff}$ obtained in Step 3b.

Step3e. The iterative loop is completed by returning to Step 3a to compute a new value of *λ* using the new value of n' from Step 3d. Iterations are continued until successive values of n' agree to within a specified tolerance.

Step 4. Calculation of τ_w

The value of τ_w is obtained from the cubic spline using the final converged value of $8V / D_{eff}$ from Step 3.

Step 5. Generalized Reynolds Number

The generalized Reynolds number is calculated using the following equation, which is obtained by combining **Eqs. 29** and **33**:

$$\mathrm{Re}_G = \frac{D_{eff}\,(8V / D_{eff})V\rho}{g_c \tau_w} \qquad \ldots(37)$$

Step 6. Friction Factors

Two friction factors are calculated, one for laminar flow (f_L) and one for turbulent flow (f_T). For turbulent flow, an extended version of the Dodge-Metzner (1959) equation that includes the effect of surface roughness is used, as given by Reed and Pilehvari (1993).

$$f_L = 16 / \mathrm{Re}_G \qquad \ldots(38)$$

$$f_T^{-0.5} = -4 \log_{10} A \qquad \ldots(39)$$

$$A = \left\{ \left(0.27\, \varepsilon / D_{eff}\right) + 1.26^{(n')^{-1.2}} \Big/ \left[\mathrm{Re}_G\, f_T^{(1-n'/2)}\right]^{(n')^{-0.75}} \right\} \qquad \ldots(40)$$

In **Eq. 39**, ε is the (absolute) surface roughness. The correct value, *f*, of the friction factor is assumed to be the larger of f_L and f_T.

Step 7. Pressure Drop
The friction factor from the previous step is used to calculate the pressure drop.

$$\Delta P = \frac{2 f \rho V^2 L}{g_c D_h} \quad \ldots(41)$$

As previously noted, **Eq. 2** is valid for values of *n* in the range 0.4 to 1.0. However, it has been found that reasonable results are obtained in the above method for values of n' as low as 0.25. Therefore, in Step 3 the value of n' is forced to be in the range 0.25 to 1.0. If a value outside this range is obtained during the iterative procedure, it is reset to either 0.25 or 1.0, whichever is closer to the computed value.

Results and Discussion

The computational procedure described above was tested using the experimental data of Subramanian (1995), who measured pressure drops for a wide variety of drilling fluids in a large flow loop operated by Amoco. The loop contained a fully eccentric annulus with inner and outer diameters of 2.375 and 5.023 inches, respectively.

Figs. 7-9 compare predicted and experimental pressure drops for three bentonite muds covering a range from low to high gel concentration. The agreement is very good in both laminar and turbulent regimes over the entire concentration range. **Figs. 10-12** show similar results for two glycol muds and a vegetable oil mud. Again, the predicted pressure drops are in close agreement with the measured values. These results are typical of a large set of cases that were tested.

Figs. 13 and **14** show results for two mixed-metal-hydroxide (MMH) muds. Here the agreement between predicted and measured values is less satisfactory. For the mud of **Fig. 13**, the agreement is reasonably good in the laminar regime and part of the turbulent regime, but there is significant under-prediction at the higher flow rates. For the mud of Fig. 14, the turbulent regime is absent, but there is significant over-prediction in the laminar regime. This result illustrates one of the limitations of the present method. MMH mud 2 exhibits extreme pseudoplastic behavior, and therefore the flow is characterized by values of n' less than 0.25. Due to the limitations of Eq. 2, however, such small values of n' are not allowed in the calculations. In fact, n' was reset to 0.25 at every flow rate for this mud, which is the reason for the over-prediction.

The above limitation notwithstanding, the overall agreement between predicted and measured pressure drops is remarkably good considering the variety of drilling fluids tested and the underlying complexity of the problem. Furthermore, the fully eccentric annulus represents the worst case from the standpoint of predictability. Therefore, the new method can be expected to provide reliable pressure drop estimates for most drilling fluids in eccentric annular geometries of practical interest.

Conclusions

The generalized hydraulic calculation method of Pilehvari and Serth (2005) has been extended to encompass flow in eccentric annuli. The new method is based on an effective diameter for eccentric annuli that includes the effects of both conduit geometry and fluid rheology. Tests on a variety of drilling fluids using data from a large flow loop indicate that the method is capable of reliably predicting the pressure drop of most drilling fluids in eccentric annuli having dimensions of practical interest.

Acknowledgments

Authors wish to acknowledge the contributions of graduate students S. Khatwani, P. Tankhiwale, and Parekh Siddharth.

References

Chhabra, R., and Richardson, J., "Non-Newtonian Flow in the Process Industries: Fundamentals and Engineering Applications", Butterworth-Heinemann, Woburn, MA (1999).

Dodge, D. and Metzner, A., "Turbulent Flow of Non-Newtonian Systems", AIChE J., **5**, p. 189 (1959).

Escudier, M. P., Oliveira, P. J. and Pinho, F. T., "Fully Developed Laminar Flow of Purely Viscous Non-Newtonian Liquids Through Annuli, Including the Effects of Eccentricity and Inner-Cylinder Rotation", Int. J. Heat and Fluid Flow, **23**, p.52 (2002).

Fang, P., Manglik, R. M. and Jog, M. A., "Characteristics of Laminar Shear-Thinning Fluid Flows in Eccentric Annular Channels", J. Non-Newtonian Fluid Mech., **84**, p.1 (1999).

Govier, G., and Aziz, K., "The Flow of Complex Mixtures in Pipes", Van Nostrand-Reinhold, New York (1972).

Guckes, T. L., "Laminar Flow of Non-Newtonian Fluids in an Eccentric Annulus", J. Eng. Ind. (Trans. ASME), **97**, p. 498 (1975).

Haciislamoglu, M. and Cartalos, U., "Practical Pressure Loss Predictions in Realistic Annular Geometries", paper SPE 28304, presented at the 69th SPE Annual Technical Conference, New Orleans, LA, 25-28 September (1994).

Haciislamoglu, M. and Cartalos, U., "Fluid Flow in A Skewed Annulus", J. Energy Res. Tech., **118**, p. 89 (1996).

Haciislamoglu, M. and Langlinais, J., "Non-Newtonian Flow in Eccentric Annuli", J. Energy Res. Tech., **112,** p. 163 (1990).

Hanks, R. W., "On the Prediction of Non-Newtonian Flow Behavior in Ducts of Noncircular Cross Section", Ind. Eng. Chem. Fund., **13**, p. 62 (1974).

Miller, C., "Predicting Non-Newtonian Flow Behavior in Ducts of Unusual Cross Section", Ind. Eng. Chem. Fund., **11**, p. 524 (1972).

Pilehvari, A., and Serth, R., "Generalized Hydraulic Calculation Method Using Rational Polynomial Model", J. Energy Res. Tech., **127**, p.15 (2005).

Reed, T. D. and Pilehvari, A. A., "A New Model for Laminar, Transitional and Turbulent Flow of Drilling Fluids", paper SPE 25456, presented at the SPE Operations Symposium, Oklahoma City, OK, 21-23 March (1993).

Reed, T. and Sas-Jaworsky II, A., "Flow of Power Law Fluids in Eccentric Annuli", paper presented at the 4th International Conference on Coiled Tubing Technology, Houston, TX, March 4-7 (1996).

Snyder, W. T. and Goldstein, G. A., "An Analysis of Fully Developed Laminar Flow in an Eccentric Annulus", AIChE J., **11**, p. 462 (1965).

Subramanian, R., "A Study of Pressure Loss Correlation of Drilling Fluids in Pipes and Annuli", M. S. Thesis, University of Tulsa (1995).

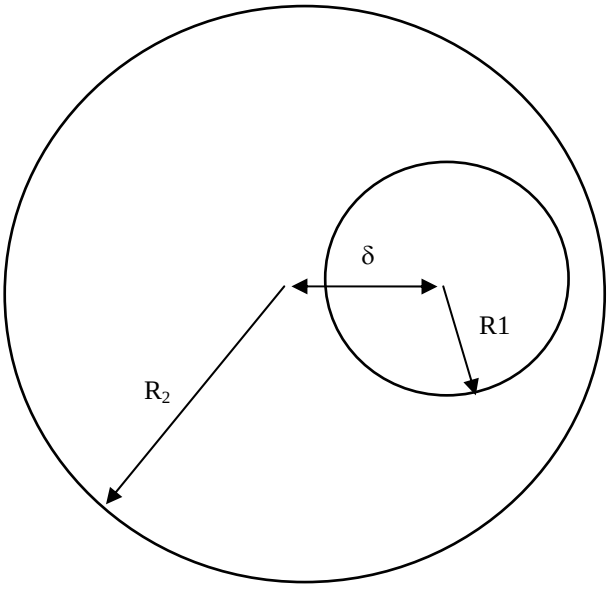

Figure 1. Cross-section of an eccentric annulus

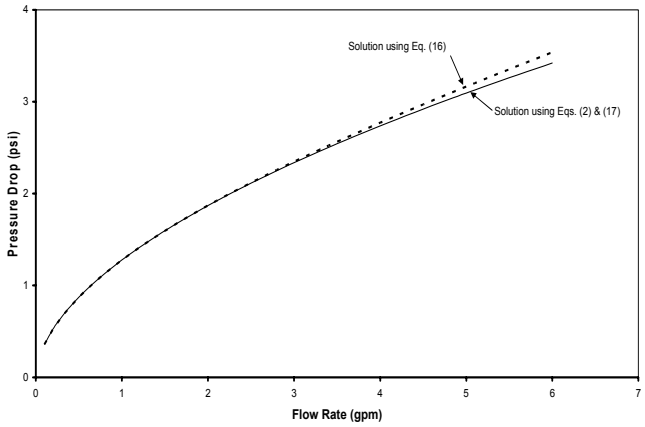

Figure 2. Test of Miller's hypothesis for a power-law fluid with n = 0.55 in a concentric annulus (e=0)

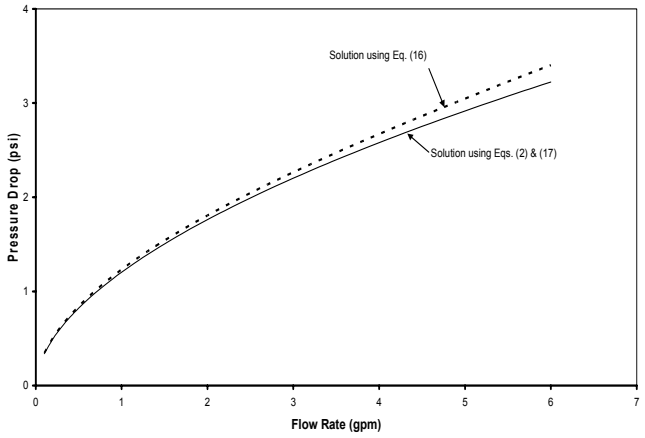

Figure 3. Test of Miller's hypothesis for a power-law fluid with n = 0.55 in an eccentric annulus (e=0.2)

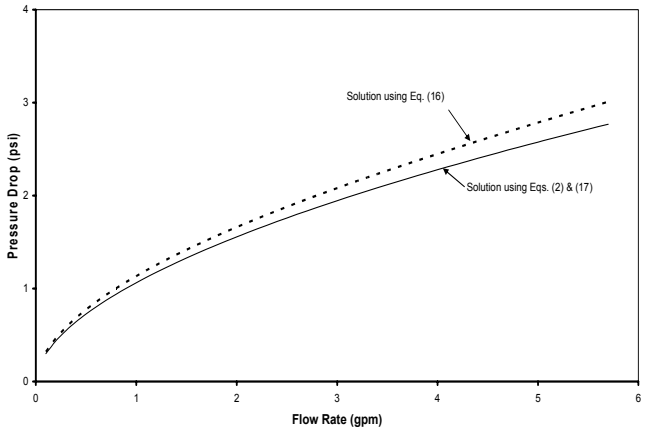

Figure 4. Test of Miller's hypothesis for a power-law fluid with n = 0.55 in an eccentric annulus (e=0.4)

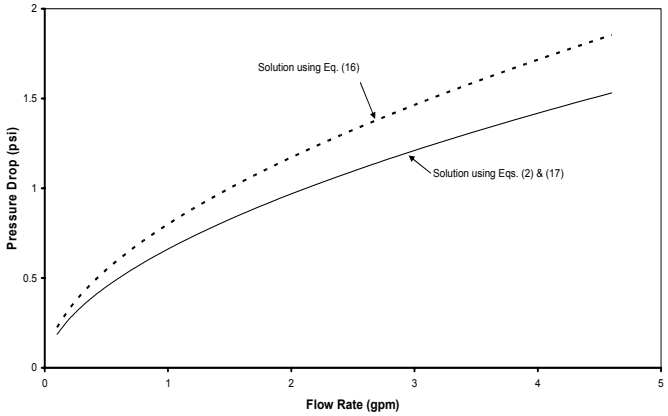

Figure 5. Test of Miller's hypothesis for a power-law fluid with n = 0.55 in an eccentric annulus (e=0.95)

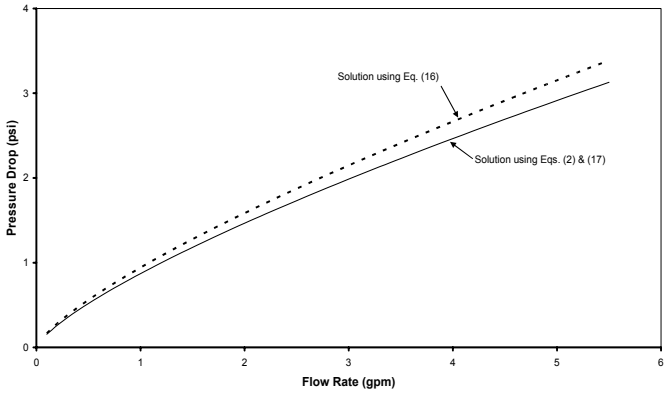

Figure 6 Test of Miller's hypothesis for a power-law fluid with n = 0.75 in an eccentric annulus (e=0.95)

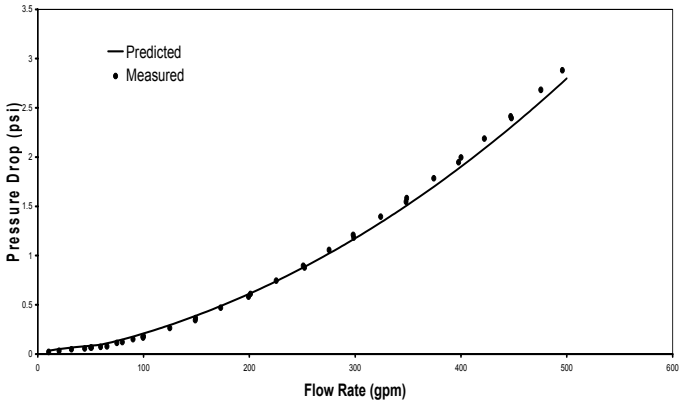

Figure 7. Predicted and measured pressure drops for Bentonite Mud 1 in a fully eccentric annulus

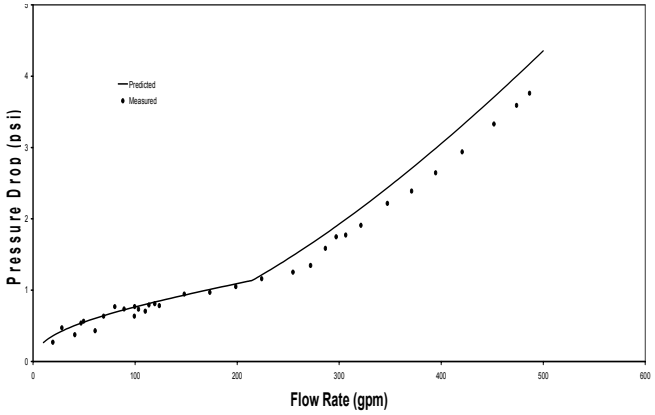

Figure 8. Predicted and measured pressure drops for Bentonite Mud 2 in a fully eccentric annulus

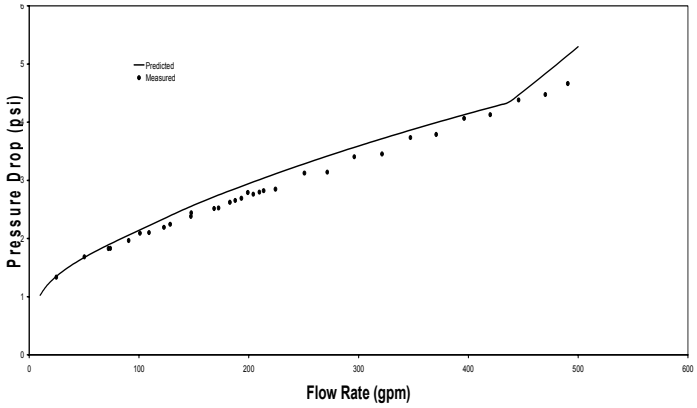

Figure 9. Predicted and measured pressure drops for Bentonite Mud 3 in a fully eccentric annulus

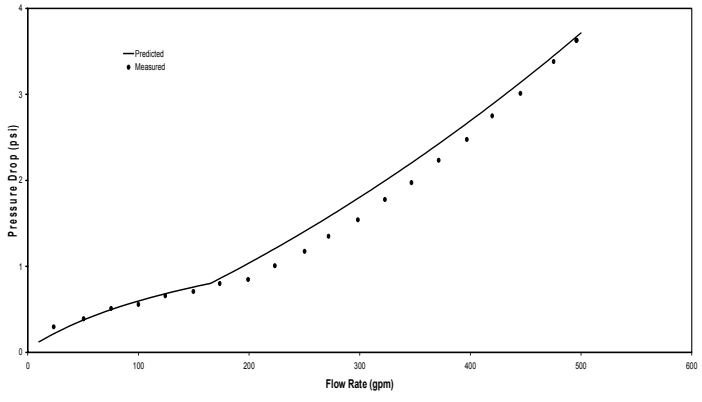

Figure 10. Predicted and measured pressure drops for Glycol Mud 1 in a fully eccentric annulus

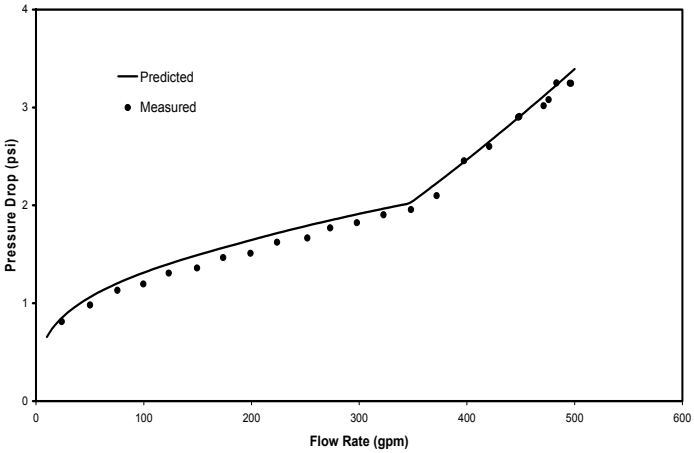

Figure 11. Predicted and measured pressure drops for Glycol Mud 2 in a fully eccentric annulus

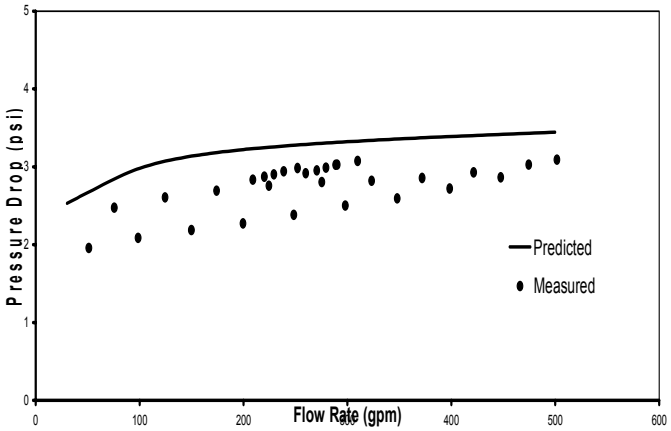

Figure 14. Predicted and measured pressure drops for MMH Mud 2 in a fully eccentric annulus

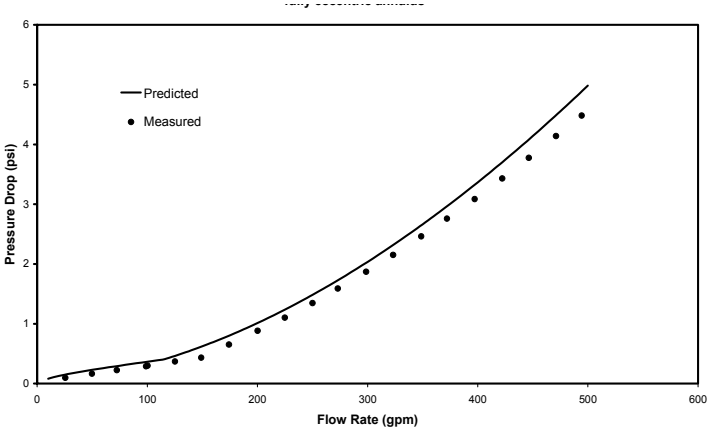

Figure 12. Predicted and measured pressure drops for Vegetable Oil Mud in a fully eccentric annulus

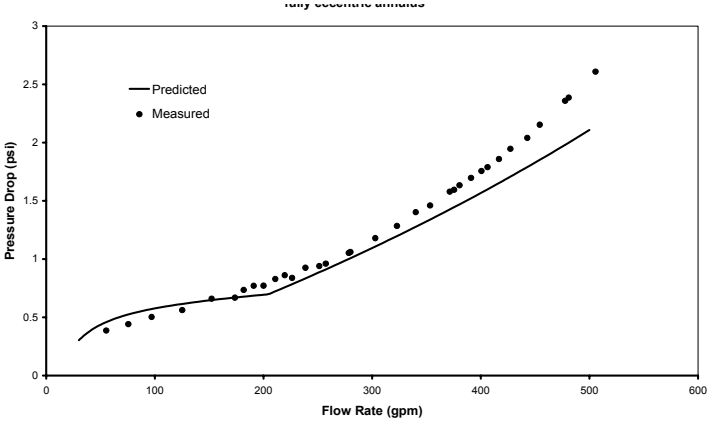

Figure 13. Predicted and measured pressure drops for MMH Mud 1 in a fully eccentric annulus